Journal of Biomedical Optics

BiomedicalOptics.SPIEDigitalLibrary.org

Laser beam coupling into nerve fiber myelin allows one to assess its structural membrane properties

Nikolay P. Kutuzov
Alexey R. Brazhe
Vladimir L. Lyaskovskiy
Georgy V. Maksimov

SPIE.

Laser beam coupling into nerve fiber myelin allows one to assess its structural membrane properties

Nikolay P. Kutuzov,[a,*] Alexey R. Brazhe,[a] Vladimir L. Lyaskovskiy,[b] and Georgy V. Maksimov[a]
[a]Moscow State University, Biophysics Department, Biological Faculty, Leninskie Gory 1/12, Moscow 119234, Russia
[b]All-Russian Research Institute for Optical and Physical Measurements, Ozernaya 46, Moscow 119361, Russia

Abstract. We show that myelin, the insulation wrap of nerve fibers, can couple laser light, thus behaving as a single-cell optical device. The effect was employed to map distinct myelin regions based on the coupling efficiency. Raman spectra acquisition allowed us to simultaneously understand the underlying microscopic differences in the membrane lipid ordering degree. The described method potentially provides new capabilities in myelin-associated disease studies and can be used as a handy tool for myelin structure investigation in combination with other methods.
 [DOI: 10.1117/1.JBO.20.5.050501]

Keywords: nerve; membranes; light coupling; Raman spectroscopy.

Paper 150135LR received Mar. 10, 2015; accepted for publication Apr. 10, 2015; published online May 8, 2015.

It is truly fascinating how the technological progress in optical instruments sometimes looks like an adoption of ideas first implemented by nature. The devices that are able to couple and transfer light comprise a huge technological field that is widely used nowadays. Remarkably, the underlying principles have already been utilized by living organisms and researchers have successfully managed to employ them in a variety of studies. Yashunsky et al. adapted the lightguide properties of an epithelial cell monolayer and by measuring its light transmission efficiency, they addressed cell–cell connectivity.[1] Probably one of the most exciting examples of a biological optical device is a Müller cell in a vertebrate retina. Franze et al. showed that the difference of refractive indices (RIs) between cell cytoplasm and the surrounding tissue allows one to guide light through a Müller cell body to the photoreceptive cell layer, avoiding the highly scattering media.[2] Here, we present a new example of a light coupling device found within a nervous system—a myelinated nerve fiber.

Sciatic nerves were dissected from a frog, Rana temporaria. Connective tissue was removed and nerve bundles were teased to obtain single fibers which were placed in the Ringer's buffer saline under a coverslip. The wide-field images of nerve fibers were obtained using the charge-coupled device (CCD) camera of an upright microscope.

A typical myelinated nerve has a cylindrical shape and at a cross section it takes the structure reminiscent of a ring-shaped optical fiber Fig. 1(a). Lipid membranes of myelin can be thought of as a dielectric core of fiber with axoplasm and the surrounding buffer as a cladding. The RIs of myelin and the surrounding buffer are approximately equal to 1.45 and 1.34 respectively, which can account for the total internal reflection on the cell/buffer interface.[3,4] Light coupling (LC) was identified as a laser spot arising from the opposite side of a fiber relative to the incident laser beam. This second spot is further designated as a focal doublet (FD) and is shown in Fig. 1 with a green arrow, whereas the incident laser beam is marked with a black arrow. It is important to mention that the studied peripheral nerve contains different types of single nerve fibers whose diameters vary considerably. We have tested the LC property of the averaged sized nerve fibers within the diameter range of $8-15\ \mu$m, where the FD was easily distinguishable.

To test whether the optical properties of myelin are similar to those of dielectric microspheres which are able to couple light, we used a simple model system—an oil drop sample. The sample was prepared by vortexing a water/immersion oil (Sigma, RI = 1.51) mixture. We compared the presence of an FD in a bud-like protrusion of a nerve Fig. 1(b) and in an oil drop Fig. 1(c), both of which have a spherical shape and approximately matching diameters. The arising FDs in both cases look very similar, which suggests that LC in a nerve fiber can possibly be due to the well-known phenomena of whispering gallery modes in dielectric microresonators.[5]

An important feature of the obtained images was the pattern of the FD: in some regions of the nerve fiber, further designated as the F-type, a bright and well-resolved FD appeared just opposite the incident focal spot as indicated by the green arrow in Fig. 1(d). The second type of the FD pattern (further referred to as the D-type) was associated with a low intensity and diffuse FD, practically indistinguishable from the image background Fig. 1(e). In order to quantify the LC and map it along a nerve fiber, we defined the following procedure. First, we chose a place on the fiber and focused the laser beam on myelin. Second, we adjusted the focus position until the maximum FD intensity was obtained, which ensured that there was no FD intensity loss due to misalignment of the incident laser beam. Third, the collected image was enhanced by histogram equalization and spatial Gaussian filtering ($\sigma = 1\ \mu$m). At each position of initial laser beam focus, shown as green squares in Figs. 1(d) and 1(e), we selected $5 \times 5\ \mu\text{m}^2$ region (shown as red squares) on the opposite side of a fiber and calculated the maximum pixel value within it. Series of images can then be obtained by moving the laser focus along the nerve fiber with a characteristic spatial step of approximately 2 μm. Finally, we were able to extract the FD intensity profile along the nerve fiber as depicted in Fig. 1(f).

The region was assigned to the F-type if the FD intensity was not less than 2 orders of magnitude higher than the image background average value. The D-type was chosen to correspond to the closest to the F-type region with an intensity of the same order as the average background value. The intermediate

*Address all correspondence to: Nikolay P. Kutuzov, E-mail: kutuzovnp@gmail.com

1083-3668/2015/$25.00 © 2015 SPIE

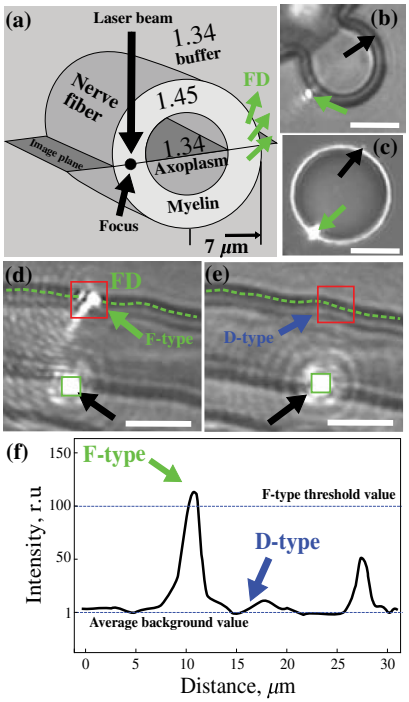

Fig. 1 (a) Schematic view of a nerve fiber with numbers corresponding to the refractive indices of the nerve and surrounding buffer solution. (b) Laser beam coupling in a bubble-like protrusion of myelin (c) and in a similar size oil drop. (d,e) Differences in light coupling properties between F- and D-type nerve regions. (f) The profile of FD intensity along the nerve fiber (f). Scale bar is 10 μm. In all images, incident laser beam and FD are marked with black and green arrows, respectively.

cases, such as the second maximum in Fig. 1(f), were also identified, but we narrowed the samples down to the F and D extreme types because they are easy to distinguish and quantify. Therefore, the value of the F-type threshold is arbitrary and was chosen so that these regions did not appear scarce along a nerve fiber and the FD intensity difference between the F-type and D-type regions was prominent.

To examine the microscopic features of myelin responsible for the difference in LC, we employed Raman microspectroscopy. This technique is convenient and widely used for lipid membrane studies.[6] A typical Raman spectra of myelin, consisting of lipid and carotenoid bands, is presented in Fig. 2(a). Peak assignment is well established in the literature.[7,8] Here, we used six main bands for calculations. Raman band intensity ratios of carotenoids and lipids allow one to study various membrane properties such as lipid chain ordering and the degree of lipid unsaturation.[9,10]

Since the focused laser light was already used to identify the F and D-type regions, we simply measured the Raman spectra in each region of interest. As a result, we obtained two sets (40 pairs) of Raman spectra for further analysis. We used a WITec alpha 300 near-field microscope with a solid-state laser (532 nm, 0.5 mW output power at sample) for image acquisition and spectroscopic measurements. Raman spectra and CCD camera images were collected with upright 20× (NA = 0.4) or 50× (NA = 0.8) objectives. We used a polarized laser beam with the polarization direction parallel to the nerve fiber axis. The FD was still clearly visible under the alternative polarization orientation; however, the one we used allowed to the collection of a more intense Raman signal. In this letter, we chose intensity ratios I_1/I_2 and Y_1/Y_2, which increase with the higher lipid ordering,[8] and the J_1/J_1 ratio, which decreases with a lower degree of fatty acids' unsaturation.[10] The spectral positions of the corresponding bands are shown in Fig. 2(a).

Our results show that the two nerve regions defined by the distinct LC properties also significantly differed in the studied ratios, as indicated in Fig. 2(b). The differences suggest that D-type myelin regions are rich in high-ordered lipid membranes. On the other hand, the F-type regions contain more of the fluid lipid phase with a higher degree of unsaturation. The interpretation of the obtained results is schematically depicted in Fig. 2(c).

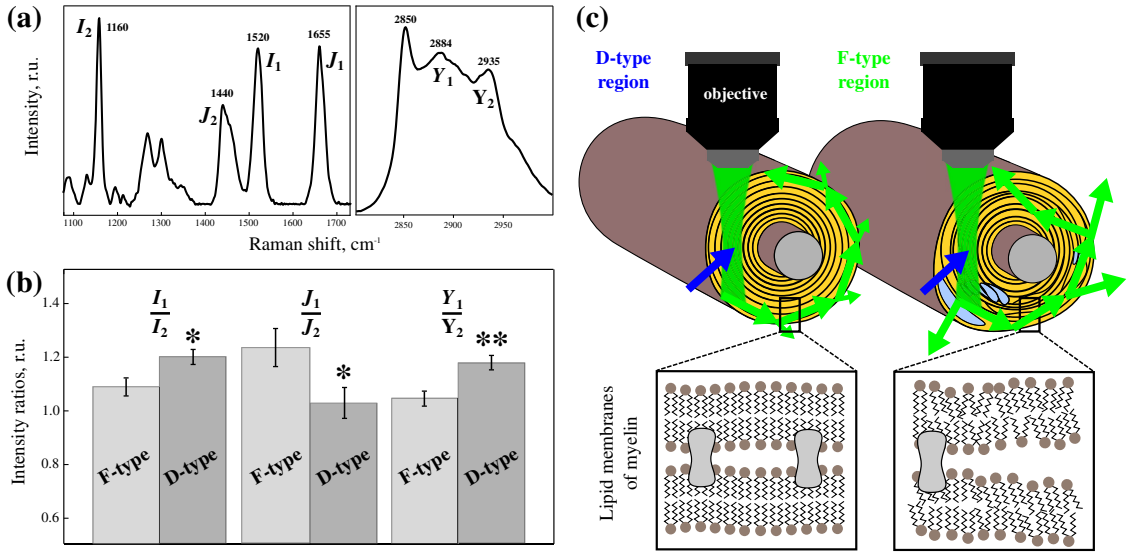

Fig. 2 (a) Typical Raman spectra of nerve fiber myelin with assignments of bands used for calculations. (b) Comparison of intensity ratios between F-type and D-type regions of myelin. (c) The interpretation of the differences in Raman spectra. Values were compared using Student *t* test, * and ** denote statistics $p < 0.05$ and $p < 0.001$, respectively.

One can speculate that it is harder for more fluid myelin regions to form densely packed membrane layers. If the layers are not rigidly packed, they can form local disorganized structures which can become the scattering centers for the incident light Fig. 2(c). On the other hand, there are known inhomogeneities in the myelin where the cytoplasmic (water) inclusions are present and the myelin layers' packing is compromised. These structures are Schmidt-Lanterman incisures (SLI), which have been known for a very long time,[11] and can be candidates for the F-type regions. However, the spacing between neighboring SLIs is usually larger than the observed distance between the F-type regions.[12] Therefore, SLI may account for some of the F-type regions, but clearly not for all of them.

An important practical application can stem from the detection of F-type regions along the nerve fiber based on the LC effect. Many demyelinating pathologies such as multiple sclerosis, acute-disseminated encephalomyelitis, and others start with local myelin reorganization.[13] Therefore, F-type regions are likely the spots of interest. The described method is simple and easy to employ as it requires only a laser coupled to a microscope equipped with a CCD camera.

In the present work, we studied the LC in the plane perpendicular to the fiber axis. Taking into account this myelin property, one can speculate that by using this effect, it is potentially possible to guide the light along the fiber length. If this is the case then the LC effect of the myelin can possibly be employed in optogenetics experiments to improve targeted light delivery to the neuron of interest. The possibility of longitudinal transfer, in our opinion, requires significant attention, and therefore, should become a subject of future studies. Summarizing, we believe that an understanding of the origin of the LC myelin properties has capabilities to advance the development of demyelination diagnostic procedures and may have important implications in the field of neuroscience.

Acknowledgments

The present work was supported by a RFBR grant for young researchers 14-04-31883. The authors have declared no conflicts of interest.

References

1. V. Yashunsky et al., "Real-time sensing of cell morphology by infrared waveguide spectroscopy," *PLoS One* **7**, e48454 (2012).
2. K. Franze et al., "Müller cells are living optical fibers in the vertebrate retina," *Proc. Natl. Acad. Sci. U.S.A.* **104**(20), 8287–8292 (2007).
3. J. Ben Arous et al., "Single myelin fiber imaging in living rodents without labeling by deep optical coherence microscopy," *J. Biomed. Opt.* **16**(11), 116012 (2011).
4. A. Brazhe et al., "Non-invasive study of nerve fibres using laser interference microscopy," *Philos. Trans. A Math. Phys. Eng. Sci.* **366**(1880), 3463–3481 (2008).
5. A. Matsko and V. Ilchenko, "Optical resonators with whispering-gallery modes-part i: basics," *IEEE J. Sel. Topics Quantum Electron.* **12**, 3–14 (2006).
6. C. Krafft et al., "Near infrared Raman spectra of human brain lipids," *Spectrochim. Acta A Mol. Biomol. Spectrosc.* **61**(7), 1529–1535 (2005).
7. M. Pézolet and D. Georgescauld, "Raman spectroscopy of nerve fibers. a study of membrane lipids under steady state conditions," *Biophys. J.* **47**, 367–372 (1985).
8. N. Kutuzov et al., "ATP-induced lipid membrane reordering in the myelinated nerve fiber identified using raman spectroscopy," *Laser Phys. Lett.* **10**(7), 075606 (2013).
9. N. Kutuzov et al., "Orientational ordering of carotenoids in myelin membranes resolved by polarized Raman microspectroscopy," *Biophys. J.* **107**, 891–900 (2014).
10. H. Wu et al., "In vivo lipidomics using single-cell Raman spectroscopy," *Proc. Natl. Acad. Sci. U. S. A.* **108**(9), 3809–3814 (2011).
11. S. M. Hall and P. L. Williams, "Studies on the 'incisures' of Schmidt-Lanterman," *J. Cell Sci.* **6**(3), 767–791 (1970).
12. R. M. Gould, A. L. Byrd, and E. Barbarese, "The number of Schmidt-Lanterman incisures is more than doubled in shiverer PNS myelin sheaths," *J. Neurocytol.* **24**(2), 85–98 (1995).
13. S. Love, "Demyelinating diseases," *J. Clin. Pathol.* **59**(11), 1151–1159 (2006).

Biographies for the authors are not available.